Transactions of the Materials Research Society of Japan 29 [3] 943-946 (2004)

Nanoporous and Low-Density Materials for Laser Produced Extreme UV Light Source

Keiji Nagai, Hiroaki Nishimura, Tomoharu Okuno, Takashi Hibino, Ryoji Matsui, YeZheng Tao, Mitsuo Nakai, Takayoshi Norimatsu, Noriaki Miyanaga, Katsunobu Nishihara, and Yasukazu Izawa
Institute of Laser Engineering (ILE) Osaka University
Fax: 81-6-6879-8778, e-mail: knagai@ile.osaka-u.ac.jp

Nanoporous and low-density tin(IV)oxide was prepared as a new target of laser produced plasma (LPP) to generate extreme ultraviolet (EUV) source at 13.5 nm in wavelength. The EUV spectra depended on the target density and laser intensity. In comparison with the spectra from bulk tin and SnO_2 powder targets, the nanoporous SnO_2 gave a narrower EUV emission band width in with the same emission intensity at 13.5 nm, below $\sim 10^{12}$ W/cm^2 laser intensity. The lower density of tin induced shorter EUV emission depth resulting in optically thin plasma formation. The nanoporous SnO_2 target has merits for 1) low target mass to reduce the cost and debris, 2) film target to treat simply and avoid reabsorption by neutral gas, and 3) narrow emission spectrum as a monochromic EUV source.
Key words: Extreme Ultraviolet (EUV), Laser produced plasma (LPP), nanoporous SnO_2, nanoparticle, low density foam

1. INTRODUCTION

Extreme Ultraviolet Lithography (EUVL, Fig.1) has been identified as one of key technologies to continue the integrated circuit manufacturing industry along the technical path most commonly referred to as the road map of the semiconductor industry. In order to print node size less than 45 nm, EUVL systems will require seamless technical relations between industry and universities. In Japan, Extreme Ultraviolet Lithography System Development Association (EUVA) was established in June 2002 under auspices of Ministry of Economy, Trade and Industry (METI) to accelerate the development of an EUV lithography system. In the fiscal year 2003, according to start of new leading project for development of EUV light source for advanced lithography technology by Ministry of Education, Culture, Sports, Science and Technology (MEXT), our institute (ILE, Osaka University) have started intensive research work on the laser-produced plasma (LLP) source. Main tasks of the project are following: 1) Establishment of databases to optimize LPP EUV light source generation, 2) Innovative target design, 3) Establishment of laser technology for commercial use in EUV lithography system [1-3].

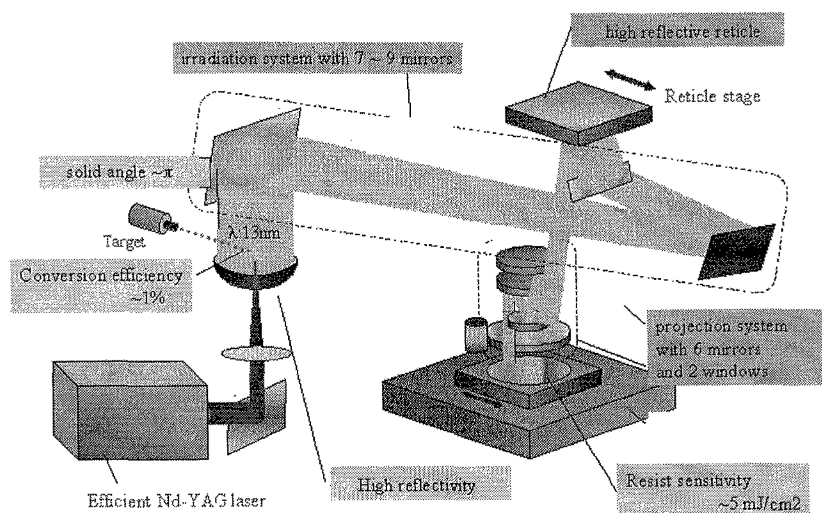

Fig. 1 EUVL system design

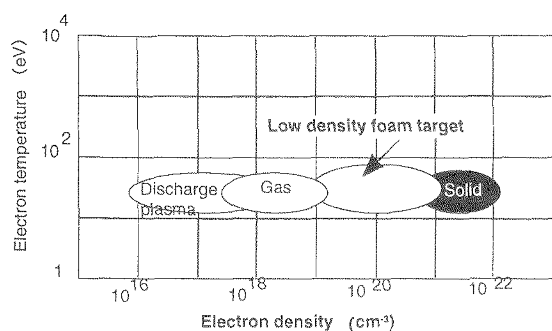

Fig. 2 Density and temperature of plasma to generate EUV emission

Target technology is one of key issues for EUV lithography system. Various types of target elements have been proposed, such as xenon [4-6], tin [1-3,7,8], lithium, silver [9], oxygen, etc. When laser incidence takes place on a target, laser energy is converted to thermal energy and the target is heated to plasma phase. A plasma is identified by element composition, temperature, and density as shown in Fig. 2, and can be controlled by the target and laser conditions. These parameters govern EUV emission from plasma. The temperature concerns valence of atom. In the case of tin target, the valence to provide EUV emission has been characterized to be ~Sn^{14+} [8]. The density governs the absorption of laser and reabsorption of EUV light (opacity effect). In the case of gas target such as xenon [4-6], conversion efficiency is not so high, even for high pressure gas. Furthermore, expansion of neutral ambient gas also decreases the efficiency due to reabortpion of EUV. In the case of solid target such as tin [1-3,7-9], laser produced plasma has a density gradient less than ~hundred micrometer. Incident laser light is absorbed at the cutoff density of ~10^{21} electrons cm^{-3}. The cutoff region is not thick, and there exist corona plasma of low density. When the corona is thick, the EUV from the cutoff is absorbed there. Furthermore, the solid target makes debris and contaminates the EUV optics.

Porous targets have a variety in density between gas, liquid, and solid, and will be innovative targets which are desired in order to attain acceptably high conversion efficiency and mitigate debris from targets (Fig. 2).

2. EXPERIMENT

Nanoporous SnO_2 was prepared by the method of Gu [10] using monodispersed polystyrene nanoparticles and liquid tin(IV)chloride. Other materials were used as received commercially. The laser irradiation and EUV monitoring systems were set as shown in Fig. 3. EUV emission spectra were measured using a grazing incidence spectrometer with observation axis of 45° with respect to the target normal. The plasma size to generate EUV light was measured using a pinhole camera through Mo/Si multilayering mirror to monitor the EUV light.

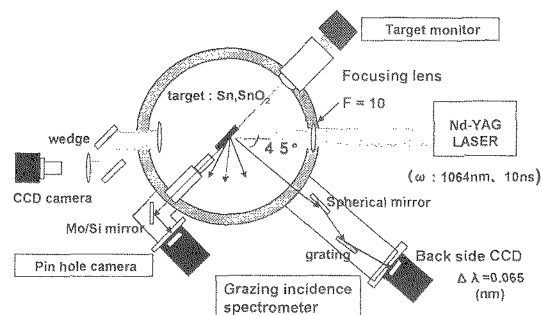

Fig. 3 EUV generation and monitoring

3. RESULTS and DISCUSSION

The porous SnO_2 mandrel had a ~200 nm pore size, which was almost same as the particle size of mandrel (Fig. 4). The average density of the nanoporous SnO_2 was 1.5 g/cm^3, which was 23% of the density of SnO_2 bulk. The density ratio well corresponds to the rest of the highest packing density (76%) of nanoparticles. The relative tin content values of powder and nanoporous SnO_2 was estimated to be 45 % and 17 % respectively per bulk tin (β phase) content.

EUV emission spectra are shown in Fig. 5. The wavelength was calibrated using line emission from highly oxidized oxygen atom (O^{5+}) as seen in Fig. 5. The bulk tin gave an emission peak at 13.4 nm and SnO_2 powder and nanostructured SnO_2 gave peaks at 13.6 nm. These peaks are almost same around 13.5 nm which is required from EUVL specification. Similar slight red shift in SnO_2 was observed by Choi et al. only for 45° and target normal axis [7], and was explained by the reabsorption by the surrounding low-density plasma (corona plasma).

The half widths of emission spectra were estimated to be 2.5 nm, 1.9 nm, and 1.0 nm for the bulk Sn, powder SnO_2, and nanoporous SnO_2, respectively. The spectra narrowing was observed in the emission depending on the density of tin; The nanoporous SnO_2 gave the narrowest bandwidth emission. The enclosed area in Fig. 5 around 13.5 nm means 2% bandwidth and will be used as monochromic EUVL light source. Other wavelength EUV light would be cut off by narrow band multi-layer mirror. From the view point reducing heat load due to absorption by the filters, the narrow emission is preferable as a EUVL light source.

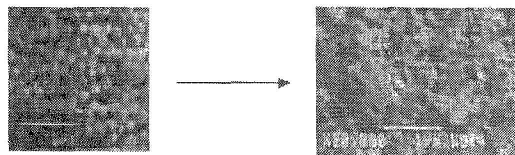

Fig. 4 SEM image of polystyrene nanoparticles (left) and a porous SnO_2 prepared from nanoparticle mandrel (right).

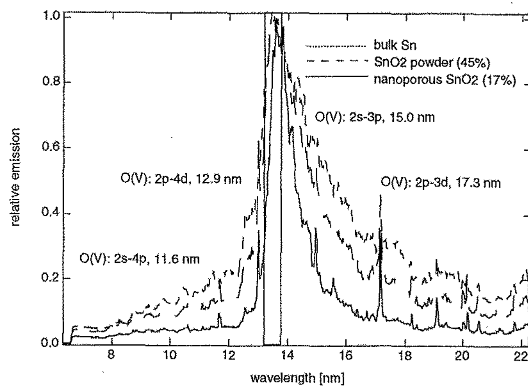

Fig. 5. EUV emission spectra from Sn and SnO_2 target. Laser incidents are fixed to be energy=500 (mJ) , pulse width = 10 (ns) , ω (1064nm) , $I_L = 5 \times 10^{11}$ (W/cm^2), and spot size = 100 × 140 (μm)$^{\Phi}$.

Conversion efficiency from laser energy to EUV emission is the most important factor to achieve the specification for the EUVL light source. Unfortunately, we did not have a calibrated energy monitor for EUV region, therefore we can compare only relative emission intensity versus laser light energy. The previous studies showed that there existed maximum in the relation. In the present case, the maximum conversion for the 13.5 nm light was obtained at 0.8 ~1.2 x 10^{12} W/cm^2. In a region of lower incident than 5 x 10^{11} W/cm^2, the emission intensity did not depend on the density of tin, and the conversion efficiency of EUV emission from laser is constant there.

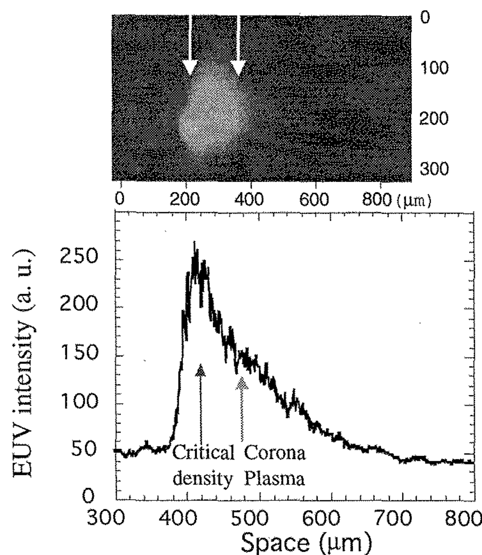

Fig. 6 EUV emission image (above) and intensity (below) from the rectangle of the target normal. Laser light was irradiated from right to the target of bulk tin. The laser intensity and spot size were 9.1 x 10^{11} W/cm^2 and 70 x 100 μm, respectively. The brightest area is close to cutoff density plasma (left arrow), and there exists corona plasma (right arrow) with low density expanding to vacuum.

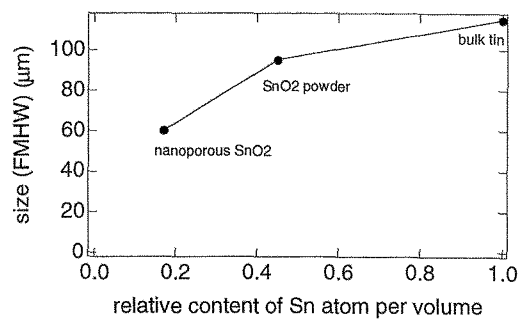

Fig. 7 EUV emission area versus initial target density obtained from EUV image shown in Fig. 6. Lower initial density (porous SnO_2) gave smaller sized EUV emission plasma.

To characterize the plasma emitting EUV light, those monochromic images through a Mo/Si mirror was observed using a pinhole camera. Figure 6 (above) shows the EUV monochromic image of a bulk tin target. Laser irradiated the target from the right side of the images. The brightest area is close to cutoff density plasma (left arrow), and there exists corona plasma (right arrow) with low density expanding to vacuum.

Figure 7 shows the dependence of EUV emission plasma size on the density; The low density of tin gave small EUV emission size. The relation can be explained by the effective plasma depth contributing to EUV emission.. In general, the laser light is absorbed at plasma with critical electron density. When the laser intensity is high, the plasma temperature at critical density becomes excessively high, and emission peak moves to shorter wavelength (<10 nm) [1, 7]. The x-ray (<10 nm) is reabsorbed by a low temperature corona plasma which surrounds the central hot region. As a result, there exists two peak of EUV emission of 1) high temperature region corresponds to critical density where shorter wavelength (<10 nm) emission is involved and 2) corona plasma region heated by the reabsorption of x-ray. On the contrary, low laser intensity gave only a heat spot at the critical density.

The mechanism of x-ray generation at critical density and reabsorption by the corena plasma also well explains the spectra narrowing for nanoporous SnO_2 target. Under optically thick plasma, observed spectrum tends to suppress the emission peak at 13.5 nm and relatively the spectral foot in the both sides of the peak becomes higher. On the other hand, effective depth of tin plasmas is thin for low density SnO_2 target, resulting in less reabsorption. As a consequence, the spectrum for the bulk tin target appears to be wider than those for the low density SnO_2 targets.

These results infers that much lower tin density will exhibit narrower spectrum with keeping the same conversion efficiency. In the field of laser-plasma physics, low density foam plastics have been widely used as matrices of heavy metal particles. [11] We have investigated a new preparation technique; An ultralow density hydrocarbon plastics foam (~2 mg/cm^3) was prepared as aerogels using density matched alcohol gels [12-15]. Figure 8 shows an example of this morphology where sub-micrometer lamella structure is observed where previous polymer matrices had large void

structure ~ 20 μm.[16] These aerogels become matrices of tin or tinoxide nanoparticles with controlling target structure such as thin film, and reduce the reabsorption due to under critical density. Further investigation is undertaken in details.

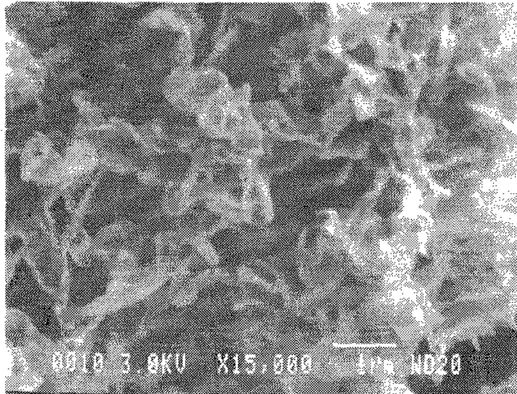

Fig. 8 SEM image of an ultralow density (2~3 mg/cm^3) poly(4-methyl-1-pentene) foam with sub-micrometer lamella structure.

4. CONCLUSIONS

Nanoporous SnO_2 prepared using nanoparticle mandrel was irradiated by 10^{11} ~ 10^{12} W/cm^2 Nd-YAG laser, and showed 13.5 nm emission with narrow band width in comparison to bulk Sn and powder SnO_2. Emission area of nanoporous SnO_2 is smaller than bulk Sn and powder SnO_2. The reason can be explained by the difference of effective EUV plasma depth and absorption of EUV light by surrounding low temperature plasmas.

A part of this work was performed under the auspices of MEXT (Ministry of Education, Culture, Science and Technology, Japan) under contract subject "Leading Project for EUV lithography source development".

REFERENCES

[1] H. Nishimura et al., In *Proceedings of Inertial Fusion Sciences and Applications 03, in press.*
[2] M. Nakai et al. In *SPIE Proceedings* vol. 5196, *in press.*
[3] N. Miyanaga et al. In *Proceedings of IEEE/LEOS 2003, in press.*
[4] A. Sasaki., *J. Plasma Fusion Res.*, **74** (2003) 315.
[5] M. Suzuki et al. *Phys. Plasma*, **10** (2003) 227.
[6] K. Kondo et al . *Appl. Surf. Sci.*, **197** (2002) 138.
[7] I. W. Choi et al., *J. Opt. Soc. Am. B*, **17** (2000) 1616.
[8] G. O'Sallivan et al., *Opt. Eng.*, **33** (1994) 3978.
[9] H. Tang et al., *Jpn. J. Appl. Phys.*, **42** (2003) 443.
[10] Z.-Z. Gu et al., *Chem. Mater*, **14** (2002) 760.
[11] W. L. Perry, et al., *Appl. Phys. Lett.* **66** (1995) 314.
[12] K. Nagai et al., "Laser Fusion Nanomaterials", In *Encyclopedia of Nanoscience and Nanotechnology, in press.*
[13] K. Nagai et al., *Jpn. J. Appl. Phys.*, **41** (2002) L431.
[14] K. Nagai et al., *Fusion Sci. Technol.*, in press.
[15] S. Okihara et al., *Phys Rev. E*, in press.
[16] M. A. Mitchell, et al., *Fusion Technol.* **28** (1995) 1844.

(Received October 10, 2003; Accepted January 31, 2004)